Distribution of Myocilin and Extracellular Matrix Components in the Juxtacanalicular Tissue of Human Eyes

Jun Ueda, Kelly Wentz-Hunter, and Beatrice Y. J. T. Yue

Purpose. To examine ultrastructurally the composition of extracellular matrix (ECM) materials, the distribution of myocilin, and the colocalization of myocilin with ECM components in the juxtacanalicular tissue (JCT) of normal human eyes.

Methods. Postembedding immunoelectron microscopic studies were performed with antibodies specific for major ECM components, including fibronectin, laminin, vitronectin, tenascin, elastin, fibrillin-1, microfibril-associated glycoprotein (MAGP)-1, decorin, versican, and five types of collagen (I, III, IV, V, and VI). Hyaluronic acid was localized with the use of biotinylated hyaluronic acid–binding protein. Colloidal gold labeling was also performed using an anti-human myocilin polyclonal antibody. Colocalization of myocilin with ECM components was examined by double labeling, using different-sized gold particles. The possible interaction between myocilin and ECM molecules was evaluated by in vitro binding assays.

Results. Amorphous basement membrane-like materials in the JCT were confirmed to be made up chiefly of collagen type IV, laminin, and fibronectin. Elastin was localized to the central core of sheath-derived plaques. Fibronectin, fibrillin-1, MAGP-1, decorin, and type VI collagen were all localized to clusters of the banded material in the sheath surrounding the core, where several types of collagen, glycoproteins, and proteoglycans were also detected. Myocilin was found to associate mainly with the sheath material, overlapping extensively in distribution with fibronectin, fibrillin-1, and MAGP-1 and moderately with decorin and type VI collagen. Its localization was distinct from that of elastin. Interactions of myocilin with molecules such as fibronectin and fibrillin-1 were confirmed biochemically.

Conclusions. This study illustrated ultrastructurally the composition of ECM materials in the JCT of normal human eyes. The key finding was the association of myocilin with microfibrillar architecture in sheath-derived plaques where pathologic changes have been documented to occur in eyes of patients with primary open-angle glaucoma. (*Invest Ophthalmol Vis Sci.* 2002;43:1068–1076)

Myocilin, previously termed the trabecular meshwork-inducible glucocorticoid response (TIGR) protein, was identified as an upregulated molecule secreted by cultured human trabecular meshwork (TM) cells after the treatment of glucocorticoids such as dexamethasone.[1,2] The time course of the myocilin induction was similar to that seen clinically as steroid-induced intraocular pressure elevation.[3] The gene was independently cloned from a retinal cDNA library and was termed "myocilin" for its significant homologies with nonmuscle myosin.[4] Recent genetic studies have linked the myocilin gene to juvenile glaucoma and primary open-angle glaucoma (POAG), and multiple mutations have been identified.[5–7] The frequency of the myocilin mutation has been reported to be approximately 2.6% to 4.6% among randomly screened patients with POAG.[7–9]

The inner wall of Schlemm's canal and the juxtacanalicular tissue (JCT), also referred to as the cribriform meshwork,[10] are believed to be largely responsible for normal aqueous humor outflow resistance.[11] There have been extensive morphologic studies, attributing the abnormal accumulation of extracellular matrix (ECM) materials in this region to the increased outflow resistance in glaucoma.[10,12–18] The ECM materials in the JCT in normal human eyes were described and distinguished by Rohen et al.[10] into amorphous basement membrane-like material and sheath-derived (SD) plaques. The former, initially called type I plaque, is made up of low electron-dense substances forming small patches and is observed primarily underneath the inner wall endothelial lining. The SD plaques, originally classified as type II and type III, encompass the electron-dense core, or the cribriform plexus, a network that forms with elastic-like fibers, and the surrounding sheath, with clusters of banded material embedded therein. Morphometric analysis has revealed that the amount of SD plaques is significantly increased in the TM of POAG-affected eyes compared with normal eyes.[19] The exact nature of these ECM structures in either normal or glaucomatous eyes has yet to be established.

In this study, we took a systematic approach to analyze the composition of ECM materials in the JCT of normal human eyes by postembedding colloidal gold immunoelectron microscopy (EM). The tissue was immunostained with antibodies specific for major ECM components of TM including fibronectin, laminin, vitronectin, tenascin, elastin, fibrillin-1, microfibril-associated glycoprotein (MAGP)-1, decorin, versican, and five types of collagen (I, III, IV, V, and VI).

The distribution of myocilin in this region was also investigated. In an earlier study, we localized myocilin ultrastructurally to both intracellular and extracellular sites in cultured human TM cells and tissues.[20] In normal TM tissues, myocilin was detected in the core of trabecular beams and the matrices in the JCT area. The present study extended our previous effort and analyzed the extracellular localization of myocilin in greater detail. More important, double labeling using different-sized gold particles[21] was performed to determine whether, and which, ECM components codistributes with myocilin in the JCT. Biochemically, in vitro binding assays were applied to assess the possible interaction of myocilin with these molecules.

From the Department of Ophthalmology and Visual Sciences, University of Illinois at Chicago College of Medicine, Chicago, Illinois.

Supported by Grants EY05628, EY03890 and Core Grant EY01792 from the National Eye Institute and the Japan Foundation for Aging and Health, Aichi, Japan.

Submitted for publication September 4, 2001; revised December 7, 2001; accepted December 20, 2001.

Commercial relationships policy: N.

The publication costs of this article were defrayed in part by page charge payment. This article must therefore be marked "*advertisement*" in accordance with 18 U.S.C. §1734 solely to indicate this fact.

Corresponding author: Beatrice Y. J. T. Yue, University of Illinois at Chicago, Department of Ophthalmology and Visual Sciences, 1855 W. Taylor Street, Chicago, IL 60612; u24184@uic.edu.

Investigative Ophthalmology & Visual Science, April 2002, Vol. 43, No. 4

Materials and Methods

Tissue Preparation

Six normal human donor eyes (donor ages, 39, 47, 48, 58, 72, and 74 years) with no history of glaucoma or other eye diseases were obtained from the Illinois Eye Bank at Chicago within 24 hours of death. Uveal tissues were removed, and the anterior segments of the eyes, including TM, were excised. The specimens were fixed at room temperature (RT) for 3 hours in 4% paraformaldehyde and 0.1% glutaraldehyde in 0.1 M phosphate buffer (pH 7.4) and were further dissected into smaller pieces (2 × 1 × 1.5 mm). After rinsing in phosphate buffered saline (PBS), the specimens were dehydrated at −20°C through a graded series of *N*, *N*-dimethylformamide (DMF). DMF was then exchanged stepwise to glycol methacrylate (GMA) embedding medium, which was made up of 65 mL 2-hydroxyethyl methacrylate, 35 mL *n*-butyl methacrylate, 5 mL ethylene glycol dimethacrylate, and 0.5 g benzoin methyl ether.[22] The specimens were subsequently polymerized by ultraviolet irradiation for 48 hours at −20°C. Ultrathin 80-nm serial sections were cut transversely through the entire layers of TM and were mounted on 150-mesh nickel grids.

Immunogold Labeling and EM Study

To identify the composition of ECM materials in the JCT, immunogold labeling was performed. Ultrathin sections were incubated for 15 minutes at RT in blocking buffer containing 1% bovine serum albumin (BSA; Sigma, St. Louis, MO) in PBS to minimize nonspecific binding. The blocking solution was removed, and the grids were incubated with the primary antibody for 3 hours at RT. The primary antibodies were rabbit anti-human fibronectin (1:20 in blocking buffer; Cappel, Aurora, OH), laminin (1:15; Sigma); tenascin (1:20; Life Technologies, Gaithersburg, MD); elastin (1:150; Elastin Products Company, Owensville, MO); fibrillin-1 (1:150; Elastin Products Company); MAGP-1 (1:200; Elastin Products Company); collagen types I (1:20; Chemicon, Temecula, CA), III (1:40; Chemicon), and IV (1:20; Collaborative Research, Bedford, MA); mouse anti-human vitronectin (1:20; Life Technologies); versican (1:15, Seikagaku Corp., Falmouth, MA); collagen types V and VI (1:15; Chemicon); and sheep anti-human decorin (1:500; United States Biological, Swampscott, MA). The optimal dilution of each antibody was determined from several preliminary tests.

A polyclonal antibody anti-myocilin was also used as a primary antibody at a dilution of 1:200. This antibody was generated in rabbits against a synthetic polypeptide corresponding to the amino acid sequences RTAQLRKANDQ (amino acids 33–43) of human myocilin. The synthetic peptide and the polyclonal antibody were prepared by Alpha Diagnostic International (San Antonio, TX). The antibody was further purified by affinity column. Using this antibody, Western blot analysis of normal human TM tissue extracts showed a characteristic 66-, 57- and 55-kDa myocilin band pattern, similar to that observed with another peptide antibody generated in our laboratory.[20] When the antibody was preadsorbed with the immunogenic peptide, none of the bands was detected.

After incubation with the primary antibody, the grids were rinsed by thorough shaking in a mixture of 0.05% Tween-20 in PBS. The sections were then incubated either with 12-nm colloidal gold–conjugated goat anti-rabbit IgG (1:50) or anti-mouse IgG (1:30) or 6-nm colloidal gold–conjugated donkey anti-sheep IgG (1:100, all from Jackson ImmunoResearch, West Grove, PA) at RT for 1 hour. The sections were then rinsed, stained with uranyl acetate and examined under a transmission electron microscope (JEM-1220; JEOL, Peabody, MA) at an 80-kV accelerating voltage. As a negative control, normal rabbit IgG or anti-myocilin preadsorbed with the immunogenic peptide was used instead.

To reveal the localization of hyaluronic acid, the sections were incubated with biotinylated hyaluronic acid–binding protein (HABP; 1:10; United States Biological) after the blocking procedure. For detection of biotinylated HABP, the sections were incubated in horseradish peroxidase (HRP)–conjugated streptavidin (1:50; Jackson ImmunoResearch) for 1 hour and further incubated in 6-nm colloidal gold–conjugated goat anti-HRP (1:20, Jackson ImmunoResearch) for 1 hour.

To examine the colocalization of myocilin with other ECM components, double labeling was performed.[21] One side of the section was immunostained with anti-myocilin and labeled with 12-nm gold particles, and the other side was stained for other ECM elements using 6-nm gold particles. Single-side incubation was achieved by floating the grids on a drop of each antibody.

In Vitro Binding Assays

To examine biochemically the interaction of myocilin with various ECM proteins, an in vitro binding assay was performed. Full-length myocilin was amplified in polymerase chain reaction (PCR) using the oligonucleotides 5′-AAAATTGTAATACGACTCACTATAGGGCGAGCCGCCACCATGTACCCATACGACGTTCCACCAATGAGGTTCTTCTGTCACGTTGC-3′ containing a T7 promoter sequence and 5′-CATCTTGGAGAGCTTGATGTCATAAGTGACC-3′. The approximately 1.5-kb myocilin PCR product was verified by DNA sequencing. In vitro translation of myocilin was performed using the TNT T7-coupled reticulocyte lysate system (Promega, Madison, WI) and ^{35}S-methionine (NEN, Boston, MA) according to the manufacturer's instructions. The translation product was analyzed by electrophoresis on a 10% sodium dodecyl sulfate-polyacrylamide gel. The gel was fixed and treated with FluoroHance (Research Products Inc., Mount Prospect, IL). A band at approximately 57 kDa, visualized using a storage phosphor system (Cyclone; Packard Bioscience, Billerica, MA), confirmed the expected ^{35}S-labeled myocilin translation product.

The following proteins were used in in vitro dot blot–binding assays: fibronectin (Collaborative Research); vitronectin (Calbiochem, San Diego, CA); laminin (Calbiochem); tenascin (Chemicon); decorin (Sigma); elastin (Elastin Products Company); keratan sulfate proteoglycan (a generous gift from James Funderburgh, University of Pittsburgh, Pittsburgh, PA); collagen types I, III, IV, and VI (all from Calbiochem); and collagen type V (Southern Biotechnology Associates, Birmingham, AL). BSA was used as a negative control, and nonradioactive in vitro–translated myocilin protein was used as a positive control.

Approximately 10 μg of each protein including both negative and positive controls were dot blotted onto nitrocellulose (Protran; Midwest Scientific, St. Louis, MO) membrane. The membrane was allowed to dry on vacuum and was blocked with 1% BSA-0.05% Tween 20-HKM (25 mM HEPES [pH 7.4], 115 mM potassium acetate, 2.5 mM magnesium chloride) buffer for 1 hour. The membrane was then incubated overnight at RT with in vitro–translated ^{35}S-labeled myocilin. After extensive washing with HKM, the membrane was air dried, and the radioactive protein spots were visualized using the storage phosphor system.

A C-terminal fragment of fibrillin-1 (amino acids 1019–1839) was also in vitro translated using the TNT T7 reticulocyte system as above but without radioactive methionine. This fibrillin-1 fragment was amplified through PCR using the oligonucleotides 5′-AAAATTGTAATACGACTCACTATAGGGCGAGCCGCCACCATGTACCCATACGACGTTCCAGATTACGCTCCACCAATGAGGTGCCAAGATTTGCGAATG-3′ containing a T7 promoter sequence and 5′-TTAATGAAGCAAAACCTGGATTTTCATCTTCAG-3′. A corneal cDNA library (Stratagene, La Jolla, CA) was used as the template. The approximately 2.5-kb amplified product was verified by DNA sequencing. After in vitro translation, the fibrillin-1 fragment along with BSA (negative control) was electrophoresed on a 7.5% SDS-polyacrylamide gel under reducing conditions and electroblotted to nitrocellulose. Binding of translated ^{35}S-labeled myocilin to the 90-kDa fibrillin-1 translation product was performed as for dot blot analysis, and the radioactive protein bands were detected as described earlier.

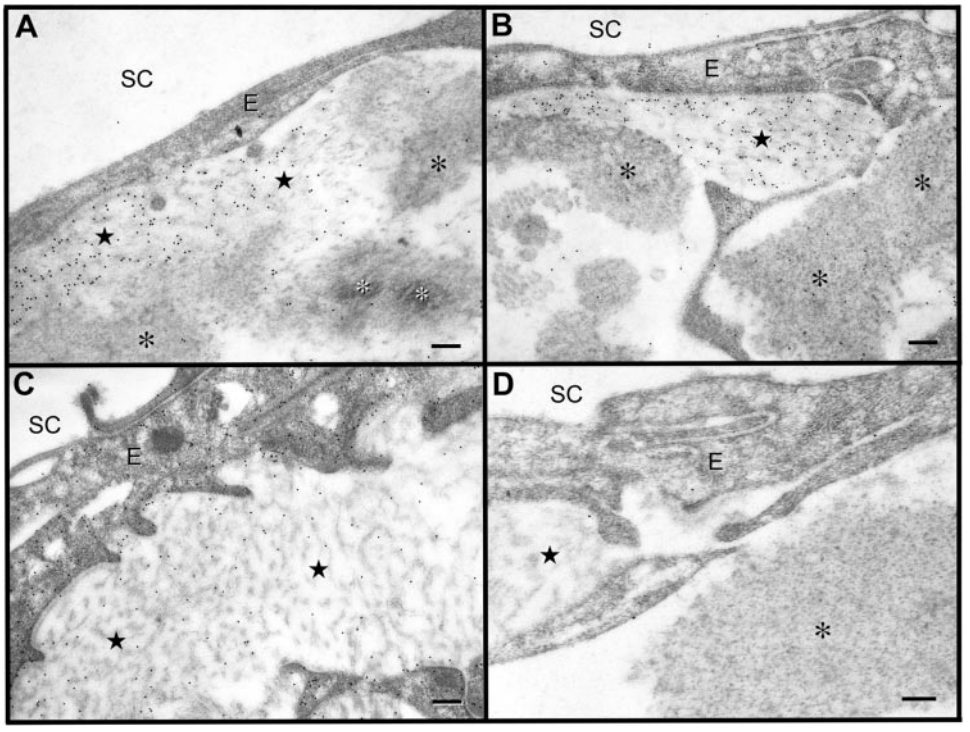

FIGURE 1. Immunogold labeling of ECM components in amorphous basement membrane-like materials (*stars*) underneath the inner wall endothelial lining of Schlemm's canal (SC) of normal human TM tissues. (**A**) Collagen type IV, (**B**) laminin, and (**C**) fibronectin. Gold particles (12 nm) extensively and specifically labeled the patchy structure of the amorphous basement-membrane–like materials. Immunogold labeling of fibronectin was also noted in the cytoplasm of the inner wall cells (E) of Schlemm's canal and JCT cells. *White asterisks* (**A**) indicate the core and *black asterisks* (**A**, **B**, **D**) the surrounding sheath of SD plaques where laminin labeling was observed. (**D**) Negative controls using normal rabbit IgG at the same protein concentration showed very scarce, nonspecific gold labeling. Bar, 200 nm.

RESULTS

Immunogold Labeling of Major ECM Components in the JCT

In normal human eyes, the typical amorphous basement membrane-like materials and SD plaques were observed by EM in the JCT region. Gold labels that represented collagen type IV were found to extensively and specifically decorate the amorphous basement membrane-like materials, the previously described masses of membranous structure approximately 60 to 100 nm thick (Fig. 1A).[18] Specific labeling to these structures was similarly observed for laminin (Fig. 1B) and fibronectin (Fig. 1C). Gold labeling of fibronectin was noted in addition in the cytoplasm of inner wall cells of Schlemm's canal and JCT cells. Such intracellular labeling has been similarly observed and reported in a recent study.[23] Very few, if any, gold particles were detected for other types of collagens, glycoproteins, proteoglycans, or hyaluronic acid. In negative controls when normal rabbit IgG at the same protein concentration was used, nonspecific gold labeling was negligible (Fig. 1D).

The core of the SD plaques, or cribriform plexus, consists of electron-dense and electron-lucent areas. In agreement with a previous report,[24] the region adjacent to the electron-lucent area was strongly immunolabeled by an antibody against elastin (Figs. 2A, 2B). This protein was barely found in the sheath area surrounding the core. Other ECM elements including fibrillin-1, MAGP-1, fibronectin, decorin, type VI collagen, vitronectin, tenascin, versican, and hyaluronic acid were observed, both in the core and the surrounding sheath that generally contained clusters of banded material with a periodicity of 100 to 110 nm. The labeling for fibrillin-1 (Fig. 3A), MAGP-1 (Fig. 3B) and fibronectin (Fig. 3C) was mostly in the sheath, with gold particles located particularly on the banded materials. Decorin (Figs. 4A, 4B) and type VI collagen (Figs. 4C, 4D) were by contrast, more abundantly distributed in the core. In the sheath, specific and strong labeling of the banded materials nevertheless was still observed (Figs. 4B, 4D). Type III collagen and laminin were found in the sheath, not in the core (photographs not shown). These molecules and others, such as vitronectin, were not linked with the banded materials, for the most part. Virtually no labels for collagen types I, IV, and V were detected, neither in the core nor the sheath (photographs not shown).

The intensity of immunogold labeling in each ECM structure or plaques was examined from more than 10 fields and was graded from ± to +++, with ± representing minimal staining,

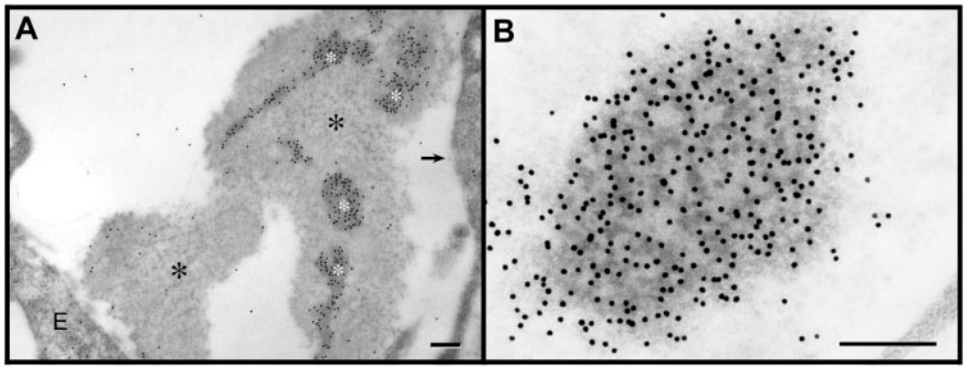

FIGURE 2. Immunogold labeling of elastin in the JCT. (**A**) The core (*white asterisks*) of SD plaques, or the cribriform plexus, was strongly immunolabeled by an antibody against elastin. By contrast, elastin was barely found in the surrounding sheath (*black asterisks*). (**B**) At a higher magnification, gold particles (12 nm) of elastin labeling were found mainly in the region adjacent to the electron-lucent areas of the cribriform plexus. (**A**, *arrow*) JCT cell. E, inner wall cell of Schlemm's canal. Bar, 200 nm.

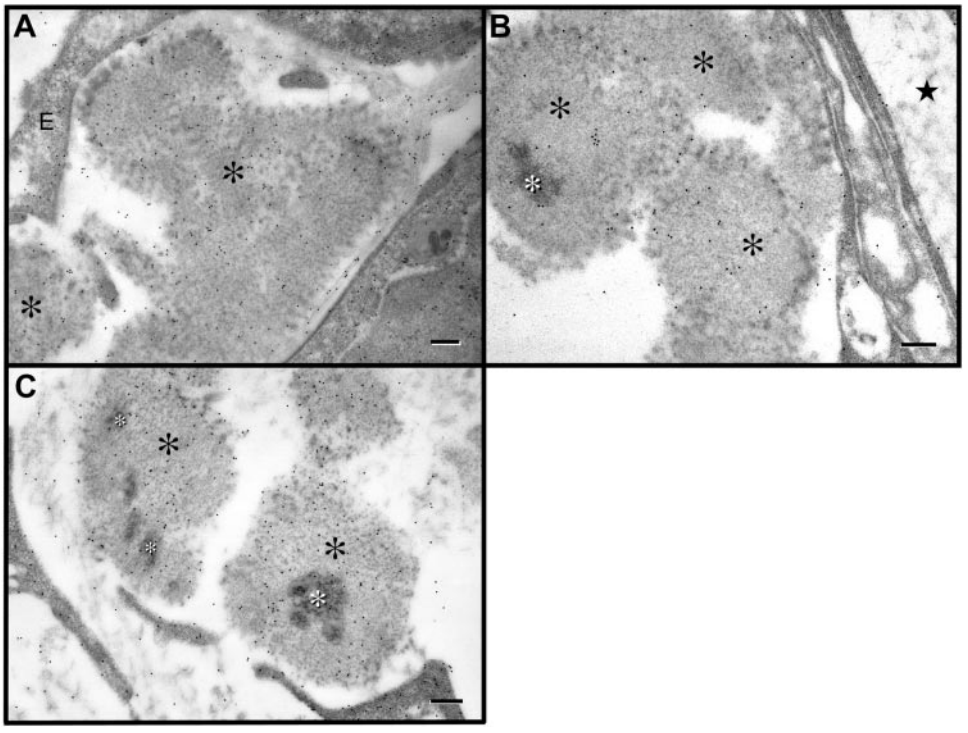

FIGURE 3. Immunogold labeling of microfibril-associated proteins in the sheath (*black asterisks*, **A–C**) and the core (*white asterisks*, **B**, **C**) of SD plaques in the JCT. (**A**) Fibrillin-1, (**B**) MAGP-1, and (**C**) fibronectin. Gold particles (12 nm) labeling fibrillin-1, MAGP-1, and fibronectin were detected both in the sheath and the core but were more abundantly distributed in the former, especially in association with the banded materials in the peripheral region. Gold particles were also found in the inner wall cells (E) of Schlemm's canal and JCT cells. (**B**, *star*) Amorphous basement-membrane–like material. Bar, 200 nm.

and + to +++, weak to intense staining. The labeling intensity and the labeling pattern for all the ECM components examined are summarized in Table 1. Results from TM tissues of six donors were essentially identical.

Immunogold Labeling of Myocilin in the JCT

Using a polyclonal antibody to myocilin, immunolabeling showed that the colloidal gold particles were heavily localized to the banded materials and other microfibrillar structures in the sheath of SD plaques (Fig. 5A). In the central core, the myocilin labeling was sparse. Gold particles representing myocilin were also at a minimum in the amorphous basement-membrane–like materials (Fig. 5B, star). This pattern of myocilin localization was similarly observed in the subendothelial region of the outer wall of Schlemm's canal (Fig. 5C). When normal rabbit IgG or the peptide-preadsorbed anti-myocilin was used instead of the primary antibody, almost no gold labeling was seen (Fig. 5D). A summary of the myocilin distribution in each type of ECM structure is also included in Table 1.

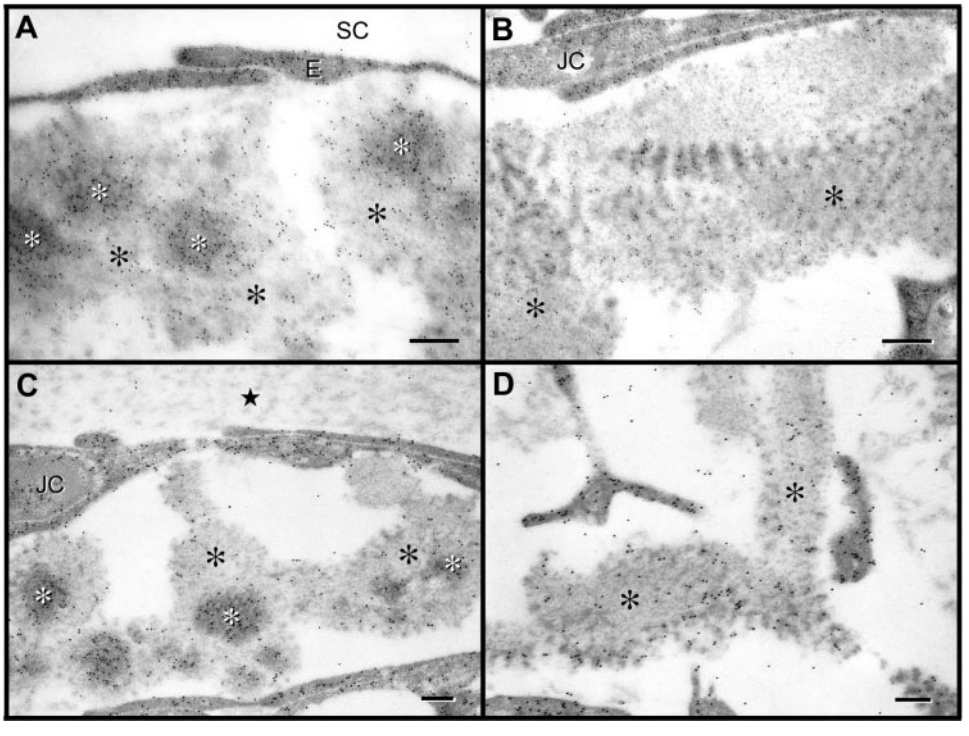

FIGURE 4. Immunogold labeling of decorin (**A**, **B**; 6 nm) and type VI collagen (**C**, **D**; 12 nm) in the sheath (*black asterisks*, **A–D**) and the core (*white asterisks*, **A**, **C**) of SD plaques in the JCT. Gold particles for decorin and type VI collagen were detected both in the sheath and the core but were more abundantly distributed in the core. In the sheath area, specific labeling of the banded materials (**B**, **D**) was observed. Gold particles were also found in the inner wall cells (E) of Schlemm's canal (SC) and JCT cells (JC). (**C**, *star*) Amorphous basement-membrane–like material. Bar, 200 nm.

TABLE 1. Immungold Labeling of ECM Components in the JCT

	Amorphous Basement-Membrane–like Materials	Core of SD Plaques	Sheath of SD Plaques	Banded Materials in the Periphery
Myocilin	±	±	++	+++
Fibronectin	++	+	++	+++
Vitronectin	±	++	++	+
Laminin	+++	±	+	+
Tenascin	±	++	++	+
Elastin	±	+++	±	±
Fibrillin-1	±	±	+	++
MAGP-1	±	±	+	++
Versican	±	++	+	+
Decorin	±	+++	++	+++
Hyaluronic acid	±	++	++	+
Type I collagen	±	±	±	±
Type III collagen	±	±	++	+
Type IV collagen	+++	±	±	±
Type V collagen	±	±	±	±
Type VI collagen	±	+++	+	++

The intensity of immunogold labeling was graded in each ECM structure or plaques from ± to +++, with ± representing minimal, and + to +++, increasingly intense staining.

Double Labeling of Myocilin and Other ECM Proteins

Immunogold double labeling with myocilin using different sized gold particles was performed. Major codistribution of myocilin (12-nm gold particles) with fibronectin (6-nm; Fig. 6A), fibrillin-1 (6-nm; Fig. 6B), and MAGP-1 (6-nm; Fig. 6C) was demonstrated. All these molecules were associated with microfibrillar architecture, especially the banded materials, in the sheath area of SD plaques. The myocilin localization also overlapped to a lesser degree and mostly in the banded material with decorin (6 nm; Fig. 6D) and type VI collagen (micrograph not shown). Minor colocalization of myocilin was also noted with other components in the sheath, such as collagen type III, laminin, versican, vitronectin, tenascin, and hyaluronic acid. The myocilin distribution however was distinct from that of elastin, and collagen types I, IV, and V. Hardly any colocalization with these proteins could be discerned.

In Vitro Binding Assays

Interactions of myocilin with various ECM components were examined biochemically. Fibronectin; vitronectin; laminin; tenascin; elastin; decorin; keratan sulfate proteoglycan; and collagen types I, III, IV, V, and VI, along with BSA (negative control) and myocilin (positive control) were dot blotted onto nitrocellulose membranes, overlaid with ^{35}S-labeled myocilin, and extensively washed. Binding or interaction of ECM pro-

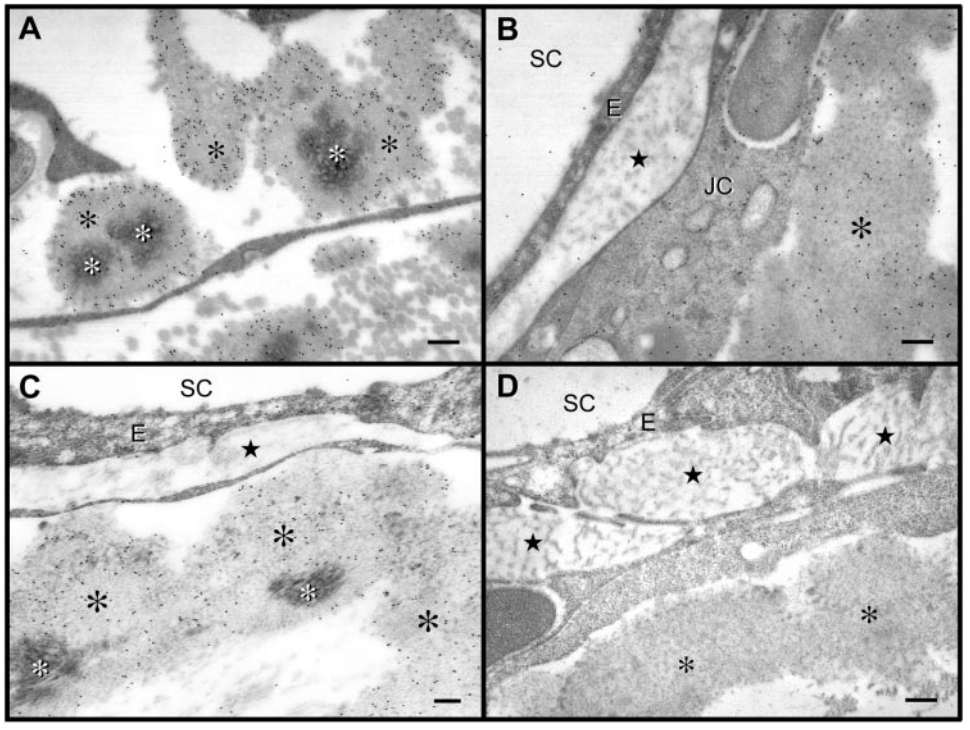

FIGURE 5. Immunogold labeling of myocilin in the JCT region of normal human TM tissues underneath the inner wall endothelial lining (E) of Schlemm's canal (SC). (**A**) Myocilin-associated 12-nm colloidal gold particles were heavily localized to the banded materials and other microfibrillar structures in the sheath (*black asterisks*, **A–D**) of SD plaques. The central core (*white asterisks*, **A**, **C**) was very sparsely labeled. (**B**) In the amorphous basement-membrane–like materials (*stars*, **B–D**), gold particles representing myocilin were scarce. (**C**) A similar pattern of myocilin localization was also observed in the subendothelial region of the outer wall of Schlemm's canal. (**D**) As a negative control, peptide-preadsorbed anti-myocilin was used to replace the primary antibody. Gold labeling was minimal. JC, JCT cells. Bar, 200 nm.

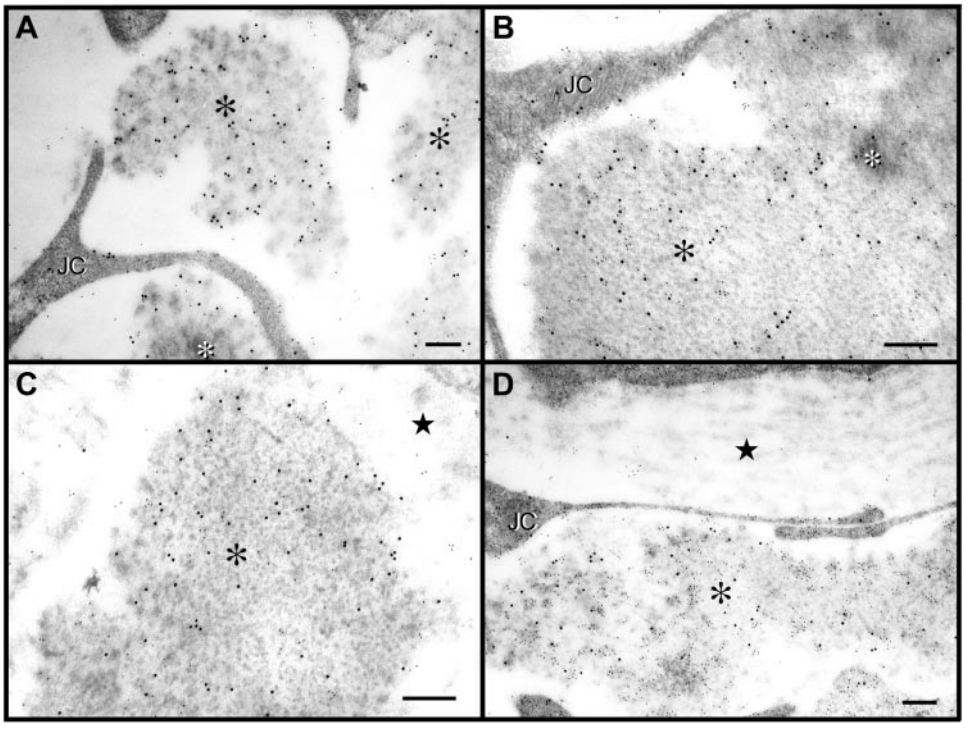

FIGURE 6. Immunogold double labeling for myocilin and ECM components in the JCT of normal human TM tissues. A major overlap in distribution between myocilin (12-nm colloidal gold particles) and fibronectin (**A**, 6-nm gold particles), fibrillin-1 (**B**, 6-nm gold particles), or MAGP-1 (**C**, 6-nm gold particles) was demonstrated. All these molecules showed microfibrillar architecture, especially the banded material, in the sheath area of SD plaques. Moderate colocalization of myocilin with decorin (**D**, 6-nm gold particles) was also noted. *White asterisks* (**A**, **B**) indicate the core and *black asterisks* (**A–D**) the surrounding sheath of SD plaques. (**C**, **D**, *stars*) Amorphous basement-membrane–like materials. JC, JCT cells. Bar, 200 nm.

teins with radiolabeled myocilin would yield dark, radioactive spots. As shown in Figure 7A, there appeared to be strong interaction of myocilin with fibronectin, laminin, decorin, collagen types I and III, and myocilin itself. Moderate-to-weak binding was seen with vitronectin, collagen types V and VI, and tenascin, whereas no interaction was observed with elastin, keratan sulfate proteoglycan, type IV collagen, and BSA. Binding to myocilin itself was expected, in that this protein has been reported previously to form dimers and oligomers[2] and was thus used as a positive control in our experiment. In addition, myocilin was found to bind to an in vitro–translated, 90-kDa C-terminal fragment of fibrillin-1 (Fig. 7B).

DISCUSSION

This is the first comprehensive study for composition of the ECM materials in normal human TM tissues by postembedding immunogold EM. We analyzed the ultrastructural distribution of three elastic fiber–associated molecules (elastin, fibrillin-1, and MAGP-1), four glycoproteins (fibronectin, vitronectin, laminin, and tenascin), two proteoglycans (decorin and versican), a glycosaminoglycan (hyaluronic acid), and five types of collagen (I, III, IV, V, and VI). An ultrastructural localization of myocilin was also completed. Although myocilin was, as previously shown,[20] also localized within the cells in association with mitochondria, vesicles, and cytoplasmic filaments, the current investigation was focused only on its extracellular localization in the JCT. Another study, with emphasis on the trabecular beams in corneoscleral meshwork, will be reported separately.

Our data indicate that the amorphous basement-membrane–like materials in the JCT are made up of major structural proteins including collagen type IV, laminin, and fibronectin. The localization of collagen type IV and laminin is consistent with that reported previously by Marshall et al.[25] The finding that fibronectin is present in the basement membrane of the inner wall of Schlemm's canal, the amorphous basement-membrane–like materials, and the sheath material of SD plaques, especially in association with the banded materials, agrees as well with the most recent data from Hann et al.[23] with the use of antigen retrieval methods.

Localization of elastin to the central core of SD plaques is consistent with that reported by Gong et al.[24] Fibrillin-1, found currently in the SD plaques, has also been noted previously in the periphery of Schlemm's canal.[26] Fibrillin-1 and -2 are major constituents of extracellular microfibrils thought to regulate the assembly and organization of elastic fibers by providing a scaffold to guide tropoelastin during organogenesis.[27] The importance of fibrillin-1 has been demonstrated by its link to Marfan syndrome, a disorder with pathologic manifestations in the skeletal and cardiovascular systems,[28] as well as ocular abnormalities, including ectopia lentis, axial myopia, presenile cataract, and POAG.[29,30] Within the microfibrillar framework, other major components including fibronectin,[31] MAGP-1 and -2,[32] decorin,[33,34] and versican[35] have also been identified. Although the mechanisms are still unclear, inroads have been made to begin the illustration of molecular mechanisms driving fibrillin polymerization and microfibril assembly.[36,37]

The present study has provided definitive evidence that MAGP-1 and fibronectin, along with fibrillin-1, are localized mostly within the peripheral mantle of the sheath surrounding the elastin core in SD plaques of the JCT, suggesting that the microfibrillar structure in this region is related in form to the elastin-associated microfibrils found particularly in tissues subjected to periodic stress, such as the respiratory and cardiovascular systems.[38] The microfibrils in the trabecular meshwork may also confer long-range elasticity required during regulation of the aqueous humor outflow.

Decorin and type VI collagen were found both in the core and sheath of SD plaques. Association with the banded material was also evident. In an ultrastructural study by Marshall et al.[39] collagen type VI was detected, but details were not attainable from the relatively poor JCT morphology, because of the cryo-ultramicrotomy technology used to retain antigenicity. Our experiments, using GMA and processing at −20°C to allow preservation of both the immunogenicity and ultrastructure, revealed a type VI collagen distribution in this region similar to that reported by Lütjen-Drecoll et al.[40]

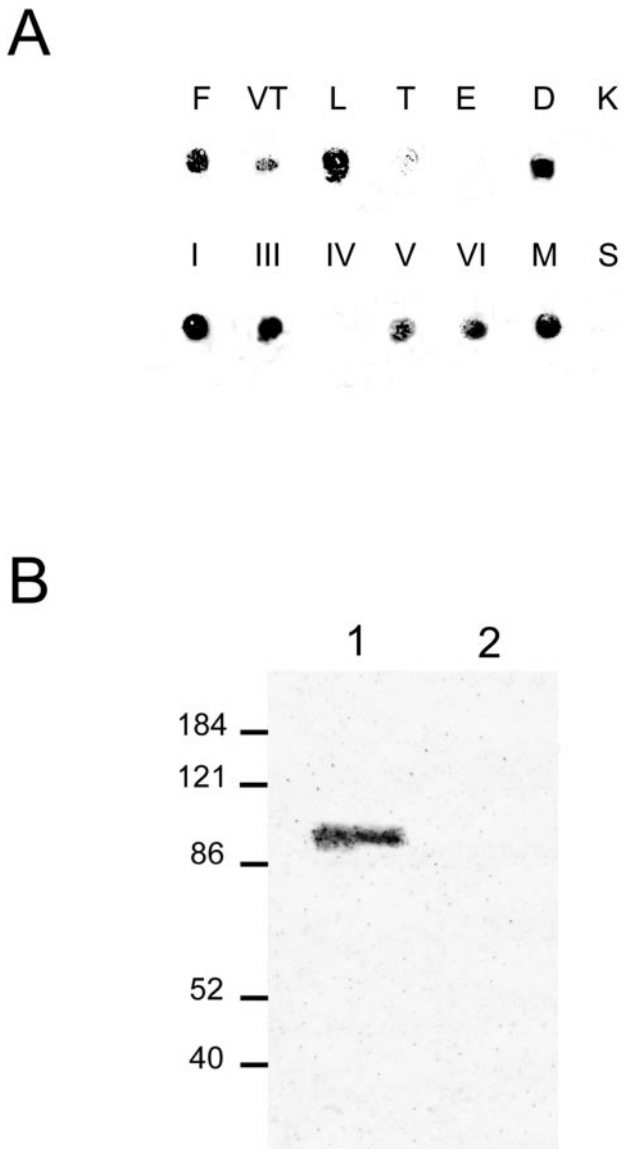

FIGURE 7. Interaction of myocilin with ECM molecules. (**A**) In vitro dot blot assays. Proteins blotted onto membranes were fibronectin (F); vitronectin (VT); laminin (L); tenascin (T); elastin (E); decorin (D); keratan sulfate proteoglycan (K); collagen types I, III, IV, V, and VI; myocilin (M); and BSA (S). After blocking, the membranes were overlaid with ^{35}S-labeled myocilin and extensively washed. Binding between myocilin and ECM proteins yielded dark, radioactive spots. Myocilin was used as a positive control and BSA as a negative control. (**B**) Binding assay with in vitro–translated fibrillin-1 C-terminal fragment. Both the approximately 90-kDa fragment (*lane 1*) and BSA (negative control, *lane 2*) were subjected to SDS-PAGE, transferred to nitrocellulose, and overlaid with ^{35}S-labeled myocilin. Radioactivity associated with the 90-kDa band indicates interaction between fibrillin-1 and myocilin.

Intracellular staining for some of the ECM molecules, such as fibronectin and decorin, was noted. This is not entirely unexpected, because ECM molecules are known to be products of cells synthesized and processed within the cells before being secreted. Intracellular labeling of ECM molecules, including collagen type I and fibronectin, has also been documented in the literature in adherent cells in culture[41] and cells in tissues.[23] There are, in addition, cases when the antibodies (for example, anti-decorin) recognize precursor molecules, resulting in abundant gold labeling in the cytoplasm of cells.

More notably, our study discloses that, besides intracellular distribution, myocilin is localized extracellularly in the JCT to the microfibrillar architecture of SD plaques, associated especially with clusters of the banded material in the peripheral region. A similar myocilin distribution pattern has also been reported recently in a study by Tawara et al.[42] using preembedding immuno-EM methods. Both of these demonstrations contradict findings in an earlier light microscopic study by Lütjen-Drecoll et al.[43] in which only intracellular staining of myocilin was seen in the TM. The difference in results may be due to the difference in methods and/or the primary antibody used.

That myocilin codistributed extensively with microfibril-associated elements including fibrillin-1, MAGP-1, and fibronectin and moderately with decorin and type VI collagen in double-labeling experiments was, by and large, expected, given the myocilin localization in SD plaques. It is, however, unknown whether myocilin is an integral constituent of the microfibrils or merely forms an association with microfibril-associated components. Interactions of myocilin with fibrillin-1, fibronectin, decorin, type VI collagen, and a few other minor SD plaque–associated proteins, such as vitronectin, laminin, and type III collagen, are confirmed biochemically by in vitro binding assays.

Dot blot assays further indicated that there was no myocilin interaction with elastin and type IV collagen, in accordance with our immunolocalization results. The results of the biochemical assays, however, also pointed toward the possibility that myocilin can interact with collagen types I and V in vitro, even though no colocalization with myocilin was seen in the EM study. The difference may simply reflect the in vitro versus the in vivo situations. It should also be noted that both these collagens are at a minimal level in the JCT and that interactions with myocilin may be very limited in any case. Laminin is another aberration that a strong myocilin interaction was detected in vitro but not observed in vivo in the amorphous basement membrane-like materials in which abundant laminin is present. It is possible that in those structures, laminin molecules interact with other ECM components, such as type IV collagen and are masked from myocilin binding.

In the TM of patients with POAG, alteration of microfibrils[44] and excessive, abnormal accumulation of SD plaques have been described in a number of EM, histologic, and immunologic studies.[10,12–18] The association of myocilin with microfibril-associated elements may be of special significance. One may speculate that myocilin participates in the microfibril assembly and overexpression, underexpression, or mutations of myocilin may alter its interaction with molecules in SD plaques, with ensuing abnormality. Gene expression by TM cells may also be disturbed and the aqueous humor outflow pathway may in turn be obstructed, leading to glaucomatous conditions.

In the eyes affected by pseudoexfoliation (PEX) syndrome, strong immunoreactivity for fibrillin-1 is found in characteristic fibrillar deposits.[26] Although the nature of the PEX material is not fully clarified, the complex glycoprotein-proteoglycan structure has been shown to contain a variety of molecules including laminin, fibronectin, fibrillin, and other elastic-fiber–associated proteins. The codistribution of myocilin with these constituent proteins suggests also a possible participation of myocilin in the formation of PEX materials. Studies of pathologic PEX tissues will shed light on this possibility.

In summary, this study demonstrates a precise localization of myocilin in the JCT. The key finding is that myocilin associates mainly with microfibril-associated elements within the banded materials in the sheath of SD plaques. This region corresponds to where pathologic changes are often observed in the eyes of patients with POAG. The present study supports

the hypothesis[45] that myocilin interacts with ECM components and may play an important role in the pathogenic mechanism of POAG.

Acknowledgments

The authors thank Kira Lathrop for expert imaging advice.

References

1. Polansky JR, Fauss DJ, Chen P, et al. Cellular pharmacology and molecular biology of the trabecular meshwork inducible glucocorticoid response gene product. *Ophthalmologica.* 1997;211:126–139.
2. Nguyen TD, Chen P, Huang WD, Chen H, Johnson D, Polansky JR. Gene structure and properties of TIGR, an olfactomedin-related glycoprotein cloned from glucocorticoid-induced trabecular meshwork cells. *J Biol Chem.* 1998;273:6341–6350.
3. Armaly MF. Effect of corticosteroids on intraocular pressure and fluid dynamics. I: the effect of dexamethasone in the normal eye. *Arch Ophthalmol.* 1963;70:482–491.
4. Kubota R, Noda S, Wang Y, et al. A novel myosin-like protein (myocilin) expressed in the connecting cilium of the photoreceptor: molecular cloning, tissue expression, and chromosomal mapping. *Genomics.* 1997;41:360–369.
5. Sheffield VC, Stone EM, Alward WLM, et al. Genetic linkage of familial open angle glaucoma to chromosome 1q21–q31. *Nat Genet.* 1993;4:47–50.
6. Stone EM, Fingert JH, Alward WLM, et al. Identification of a gene that causes primary open angle glaucoma. *Science.* 1997;275:668–670.
7. Alward WL, Fingert JH, Coote MA, et al. Clinical features associated with mutations in the chromosome 1 open-angle glaucoma gene. *N Engl J Med.* 1998;338:1022–1027.
8. Wiggs JL, Allingham RR, Vollrath D, et al. Prevalence of mutations in TIGR/Myocilin in patients with adult and juvenile primary open-angle glaucoma. *Am J Hum Genet.* 1998;63:1549–1552.
9. Fingert JH, H'eon E, Liebmann JM, et al. Analysis of myocilin mutations in 1703 glaucoma patients from five different populations. *Hum Mol Genet.* 1999;8:899–905.
10. Rohen JW, Futa R, Lütjen-Drecoll E. The fine structure of the cribriform meshwork in normal and glaucomatous eyes as seen in tangential sections. *Invest Ophthalmol Vis Sci.* 1981;21:574–585.
11. Lütjen-Drecoll E. Functional morphology of the trabecular meshwork in the primate eyes. *Prog Retinal Eye Res.* 1998;18:91–119.
12. Rohen JW, Witmer R. Electron microscopic studies on the trabecular meshwork in glaucoma simplex. *Graefes Arch Klin Exp Ophthalmol.* 1972;183:251–266.
13. Lee WR, Grierson I. Relationships between intraocular pressure and the morphology of the outflow apparatus. *Trans Ophthalmol Soc UK.* 1974;94:430–449.
14. Lütjen-Drecoll E, Futa R, Rohen JW. Ultrahistochemical studies on tangential sections of the trabecular meshwork in normal and glaucomatous eyes. *Invest Ophthalmol Vis Sci.* 1981;21:563–573.
15. Rohen JW. Why is intraocular pressure elevated in chronic simple glaucoma? Anatomical consideration. *Ophthalmology.* 1983;90:758–765.
16. Alvarado JA, Yun AJ, Murphy CG. Juxtacanalicular tissue in primary open-angle glaucoma and in nonglaucomatous normals. *Arch Ophthalmol.* 1986;104:1517–1528.
17. Rohen JW, Lütjen-Drecoll E, Flügel C, Meyer M, Grierson I. Ultrastructure of the trabecular meshwork in untreated cases of primary open-angle glaucoma (POAG). *Exp Eye Res.* 1993;56:683–692.
18. Lütjen-Drecoll E, Rohen JW. Morphology of aqueous outflow pathways in normal and glaucomatous eyes. In: Ritch R, Shields MB, Krupin T, eds. *The Glaucomas*. 2nd ed. St. Louis, MO: Mosby-Year Book; 1996:89–123.
19. Lütjen-Drecoll E, Shimizu T, Rohrbach M, Rohen JW. Quantitative analysis of "plaque material" in the inner- and outer wall of Schlemm's canal in normal- and glaucomatous eyes. *Exp Eye Res.* 1986;42:443–455.
20. Ueda J, Wentz-Hunter KK, Yue BYJT. Ultrastructural localization of myocilin in human trabecular meshwork cells and tissues. *J Histochem Cytochem.* 2000;48:1321–1329.
21. Bendayan M. Double immunocytochemical labeling applying the protein A-gold technique. *J Histochem Cytochem.* 1982;30:81–85.
22. Spaur RC, Moriarty GC. Improvement of glycol methacrylate. I: its use as an embedding medium for electron microscopic studies. *J Histochem Cytochem.* 1977;25:163–174.
23. Hann CR, Springett MJ, Johnson DH. Antigen retrieval of basement membrane proteins from archival eye tissues. *J Histochem Cytochem.* 2001;49:475–482.
24. Gong H, Trinkaus-Randall V, Freddo TF. Ultrastructural immunocytochemical localization of elastin in normal human trabecular meshwork. *Curr Eye Res.* 1989;8:1071–1082.
25. Marshall GE, Konstas AG, Lee WR. Immunogold localization of type IV collagen and laminin in the aging human outflow system. *Exp Eye Res.* 1990;51:691–699.
26. Schlotzer-Schrehardt U, von der Mark K, Sakai LY, Naumann GO. Increased extracellular deposition of fibrillin-containing fibrils in pseudoexfoliation syndrome. *Invest Ophthalmol Vis Sci.* 1997;38:970–984.
27. Mecham RP, Davies EC. Elastic fiber structure and assembly. In: Yurchenco PD, Birk DE, Mecham RP, eds. *Extracellular Matrix Assembly and Structure*. New York: Academic Press; 1994:281–314.
28. Ramirez F, Lee B, Vitale E. Clinical and genetic associations in Marfan syndrome and related disorders. *Mt Sinai J Med.* 1992;59:350–356.
29. Dietz HC, Pyeritz RE. Mutations in the human gene for fibrillin-1 (FBN1) in the Marfan syndrome and related disorders. *Hum Mol Genet.* 1995;4:1799–1809.
30. Wheatley HM, Traboulsi EI, Flowers BE, et al. Immunohistochemical localization of fibrillin in human ocular tissues: relevance to the Marfan syndrome. *Arch Ophthalmol.* 1995;113:103–109.
31. Schwartz E, Goldfischer S, Coltoff-Schiller B, Blumenfeld O. Extracellular matrix microfibrils are composed of core proteins coated with fibronectin. *J Histochem Cytochem.* 1985;33:268–274.
32. Gibson MA, Sandberg LB, Grosso LE, Cleary EG. Complementary DNA cloning establishes microfibril-associated glycoprotein (MAGP) to be a discrete component of the elastin-associated microfibrils. *J Biol Chem.* 1991;266:7596–7601.
33. Kielty CM, Whittaker SP, Shuttleworth CA. Fibrillin: evidence that chondroitin sulphate proteoglycan are components of microfibrils and associate with newly synthesized monomers. *FEBS Lett.* 1996;386:169–173.
34. Trask BC, Trask TM, Broekelmann T, Mecham RP. The microfibrillar proteins MAGP-1 and fibrillin-1 form a ternary complex with the chondroitin sulphate proteoglycan decorin. *Mol Biol Cell.* 2000;11:1499–1507.
35. Zimmermann DR, Dours-Zimmermann MT, Schubert M, Bruckner-Tuderman L. Versican is expressed in the proliferating zone in the epidermis and in association with the elastic network of the dermis. *J Cell Biol.* 1994;124:817–825.
36. Wess TJ, Purslow PP, Sherratt MJ, Ashworth J, Shuttleworth CA, Kielty CM. Calcium determines the supramolecular organization of fibrillin-rich microfibrils. *J Cell Biol.* 1998;141:829–837.
37. Gayraud B, Keene DR, Sakai LY, Ramirez F. New insights into the assembly of extracellular microfibrils from the analysis of the fibrillin 1 mutation in the *Tight skin* mouse. *J Cell Biol.* 2000;150:667–679.
38. Cleary EG, Gibson MA. Elastin-associated microfibrils and microfibrillar proteins. *Int Rev Connect Tissue Res.* 1993;10:97–109.
39. Marshall GE, Konstas AGP, Lee WR. Immunogold ultrastructural localization of collagens in the aged human outflow system. *Ophthalmology.* 1991;98:692–700.
40. Lütjen-Drecoll E, Rittig M, Rauterberg J, Jander R, Mollenhauer J. Immunomicroscopical study of type VI collagen in the trabecular meshwork of normal and glaucomatous eyes. *Exp Eye Res.* 1989;48:139–147.

41. Kuznetsov SA, Mankani MH, Gronthos S, Satomura K, Bianco P, Gehron Robey P. Circulating skeletal stem cells. *J Cell Biol.* 2001; 153:1133–1139.
42. Tawara A, Okada Y, Kubota T, et al. Immunohistochemical localization of MYOC/TIGR protein in the trabecular tissue of normal and glaucomatous eyes. *Curr Eye Res.* 2000;21:934–943.
43. Lütjen-Drecoll E, May CA, Polansky JR, et al. Localization of the stress proteins αB crystalline and trabecular meshwork inducible glucocorticoid response protein in normal and glaucomatous trabecular meshwork. *Invest Ophthalmol Vis Sci.* 1998;39:517–525.
44. Umihira J, Nagata S, Nohara M, Hanai T, Usuda N, Segawa K. Localization of elastin in the normal and glaucomatous human trabecular meshwork. *Invest Ophthalmol Vis Sci.* 1994;35:486–494.
45. Johnson DH. Myocilin and glaucoma: a TIGR by the tail? *Arch Ophthalmol.* 2000;118:974–978.
46. Clark AF, Steely HT, Dickerson JE, et al. Glucocorticoid induction of the glaucoma gene MYOC in human and monkey trabecular meshwork cells and tissues. *Invest Ophthalmol Vis Sci.* 2001;42: 1769–1780.